Control of PWM Voltage Inverters in the Pulse Dropping Region

Russel J. Kerkman, Timothy M. Rowan, David Leggate, and Brian J. Seibel

With pulse width modulated (PWM) inverter control of ac induction motors well established, attention now focuses on problems that until recently were either overlooked or deemed inconsequential. Following the groundbreaking work of Stemmler, others followed with improvements in the basic PWM strategy to increase fundamental output voltage or, in the case of Plunket, apply the basic principles to current-regulated PWM (CRPWM) inverters [1-3].

Recently, investigators observed severe instabilities with volts per hertz drives (V/Hz). The cause of the instabilities is the dead time necessary to prevent shoot-through of an inverter leg. Thus, the control designer was faced with an instability induced by a nonlinearity introduced by device requirements. This dead time or turn-on delay instability was addressed by numerous researchers [4, 5].

Problems with CRPWM inverters resulted in attempts at improving the performance of the controllers, but these improvements were marginal until the fundamental problem was analyzed and solved [6]. Prior work had ignored that ac current regulation is a type-two control problem; thus, a first-order Proportional-Integral (PI) compensator is inadequate. Simple hysteretic controllers, which operate on the instantaneous current error, lack the performance of the synchronous current regulator. Predictor/corrector controllers require additional knowledge about the load to approach the performance of the simple synchronous PI controller.

Finally, the pulse dropping region is becoming a topic of considerable interest [7-9]. Early investigations showed the difficulty in achieving the maximum voltage of the inverter once the commanded line to neutral peak voltage exceeded one-half of the dc bus voltage. This resulted in the development of third harmonic and space vector modulation techniques. In the case of CRPWM inverters, the pulse dropping region presents significant problems for the control engineer. This region was modeled, analyzed, and experimentally investigated by Rowan et al. [10]. Their results demonstrated the inherent advantage the synchronous PI controller has in the overmodulation region.

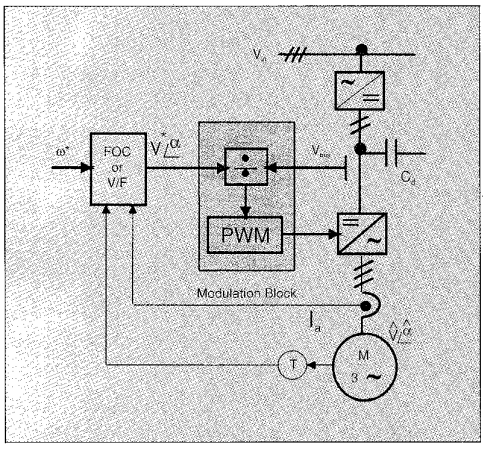

Fig. 1. System block diagram.

The authors have shown that proper control in the overmodulation region is critical for proper application of V/Hz and CRPWM inverter drives [11, 12]. Other investigators have also observed the importance of designing a controller that transitions smoothly from PWM control to six-step operation [7, 8]. Griva et al., like Holtz, proposes a technique by which switching times are calculated for the overmodulation region. While Holtz's technique completes the transition to six-step, Griva's method does not fully transition to six-step operation. Neither discussion adequately explains the

This article appeared in its original form at the 1994 Applied Power and Electronics Conference (APEC). *The authors are with Allen-Bradley Co., Standard Drives Business, 6400 W. Enterprise Drive, P.O. Box 760, Mequon, WI 53092, telephone 414-242-8263, fax 414-242-8300. All are IEEE Members; Kerkman is a Senior Member.*

The compensated modulation preamplification factor, M_{CMI}, is calculated off-line and stored in memory. An algorithm clarifying the technique for generating the table of preamplification factors is shown below. The incremental address, i, is specified by Equation (3). The table entries are calculated by an iterative loop. The loop error is given by the normalized voltage command and the fundamental component (Equation (2)). If the error is greater than or equal to ε then the error is scaled by δ, the intermediate result M'_i adjusted, and the error recalculated. If the error is less than ε then convergence is attained for table entry i. The preamplification factor $M_{CMI(i)}$ is calculated and stored. The table entry variable is incremented. If the table entry is less than the maximum, repeat the table calculation. If the table entry is larger than i_{max}, then the table is complete.

method of controlling the fundamental component of the terminal voltage.

Some of the earliest work in modeling the overmodulation region culminated in the development of a simplified model for the inverter [13]. The model provided for the transitioning from PWM to six-step operation in a V/Hz drive. Although approximate, the technique is closed-form and compatible with the processing capability of then-existent microprocessors.

Recently, the authors addressed the limitations of the approximate method [11, 12]. The compensated modulation technique (CMT) resulted from that investigation. This technique eliminates the approximation of [13] through a simple lookup table algorithm (see box). The result is a linear input-to-output voltage transfer function from PWM to six-step operation of the inverter.

This article explores in detail the operation of PWM inverters in the pulse dropping or overmodulation region. A discussion of the improvement obtained from the CMT method when compared to the previous approximate approach demonstrates a remarkable improvement in accuracy. A review of space vector overmodulation techniques reveals the similarities and differences with sine wave overmodulation. Finally, simulation and experimental results demonstrate the CMT's accuracy and controlled transition throughout the operating regions of V/Hz and CRPWM inverters.

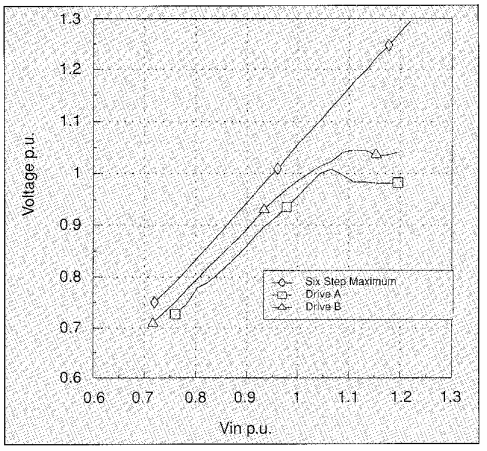

Fig. 2. Voltage characteristics for two V/Hz drives.

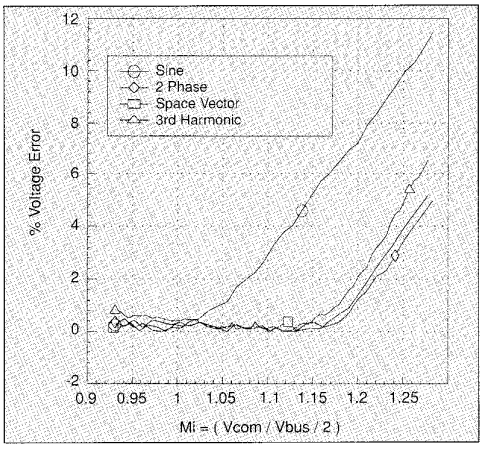

Fig. 3. Error voltage for various modulation strategies.

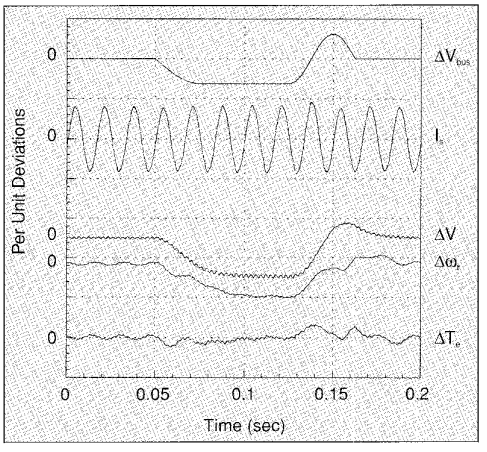

Fig. 4. V/Hz transients for bus disturbance.

Steady State and Transient Operation

Fig. 1 presents a block diagram of an ac motor drive system. Whether for high performance, where a position feedback device provides rotor position information, or V/Hz drives, the inner control remains functionally identical—a PWM switching algorithm. High-performance applications often employ a current regulator, the output serving as the voltage command to the PWM generator. A

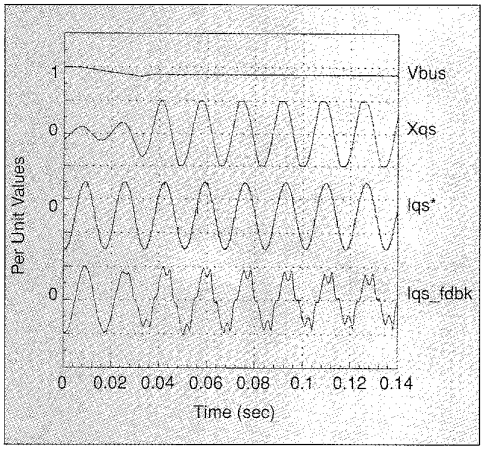

Fig. 5. CRPWM experimental results for bus disturbance.

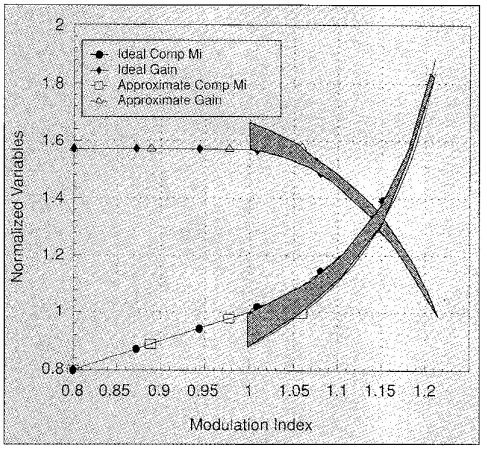

Fig. 6. Error in the approximate solution.

V/Hz drive tailors the voltage profile to the application—a linear ramp with automatic boost for high breakaway torque applications, an s-curve for fan applications. Most drives also sense the link voltage for the purposes of protection and bus voltage disturbance rejection.

Steady State

The inverter's characteristics play a significant role in establishing the performance of an ac drive. The V/Hz market requires a PWM algorithm that delivers the desired fundamental voltage ($V^*\angle\alpha$) to the motor $\hat{V}\angle\hat{\alpha}$ and ensures stable operation. In addition, control enhancements for improving the performance of the drive depend on the quality of the PWM algorithm. For example, effort spent on selective harmonic elimination is wasted if the adverse effects of dead time or turn-on delay are not corrected.

Consider the voltage characteristics for two commercially available V/Hz drives as a function of the input line voltage in Fig. 2. With rated load torque applied to each motor drive tested, the per-unit

Effort spent on selective harmonic elimination is wasted if the adverse effects of dead time or turn-on delay are not corrected.

motor voltage and current were measured as the input voltage varied as shown. Drive A maintained rated voltage for input voltages greater than 1.04 p.u., but produced less than rated output between 0.95 and 1.04 p.u. Drive B produced rated output voltage at rated input voltage, but applied excessive voltage for inputs greater than 1 p.u. Drive B exhibited better low-voltage capability than drive A by reducing the gap between the theoretical maximum (six-step) and the actual voltage delivered; however, both drives exhibit deficiencies. Even at voltage levels that would yield rated voltage within the six-step limit, each motor required more than rated current to deliver rated load [11].

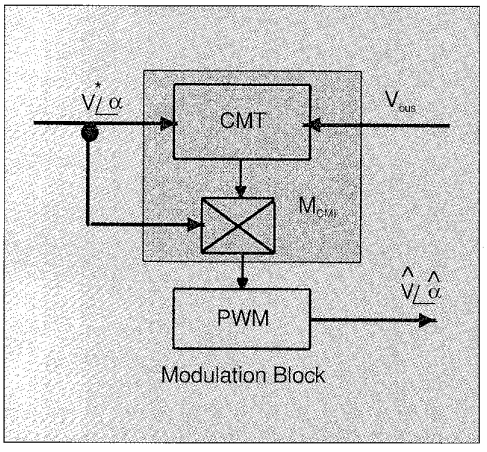

Fig. 7. Simplified implementation of the CMT.

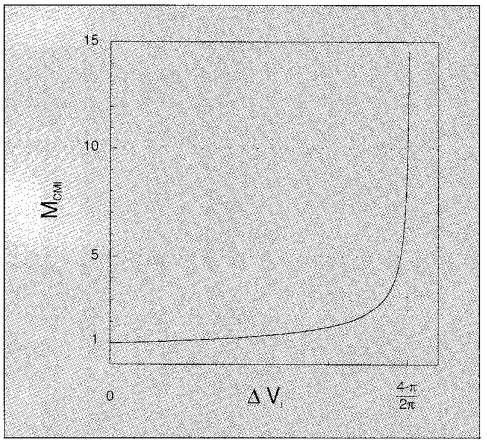

Fig. 8. Preamplification factor (M_{CMI}) versus voltage increment.

Drive A employs a third harmonic modulation strategy and drive B a two-phase discontinuous strategy. Fig. 3, which plots the normalized voltage error—$\frac{V^*\angle\alpha - \hat{V}\angle\hat{\alpha}}{V^*\angle\alpha}$—versus the modulation index for a number of modulation strategies, including those of Fig. 2, shows each modulation strategy has an associated error function. As shown in [11, 12], each modulation method has a distinct nonlinear gain characteristic in the pulse dropping region. Thus, operation within this region and the transition to six-step operation requires an overmodulation strategy that compensates for the gain characteristics of each modulation method.

Transient

The performance of a drive is often determined by its ability to reject outside disturbances. Bus voltage disturbance rejection is an important characteristic, even for V/Hz drives.

Consider the results of a computer simulation for a V/Hz drive when subjected to ±5% bus variation, as shown in Fig. 4. Nominal input voltage corresponds to a modulation index of 1.21 in Fig. 3. The top trace is the normalized bus voltage deviation from nominal (Δ Vbus); the second trace is the motor phase current (I_s); the third trace is the normalized motor terminal voltage deviation (ΔV); the fourth trace is the speed deviation ($\Delta\omega r$); the fifth trace is the normalized torque deviation (ΔT_e). It is important to note that the speed and terminal voltage exhibit an error before the disturbance—a result of the space vector algorithm's nonlinear transfer function $\frac{\hat{V}\angle\hat{\alpha}}{V^*\angle\alpha^*}$ in the pulse dropping region [12].

Once the transient begins, the terminal voltage is disturbed. The motor's response is to develop more slip to deliver the load; thus, the speed decreases, and it, together with the torque, oscillates at the characteristic frequency. This uncontrolled response is a result of a deficiency in the overmodulation strategy. The disturbance migrates throughout the drive system, acting as a perturbation to the process, which is an undesirable condition in many applications.

Fig. 5 shows experimental results of a CRPWM field-oriented induction motor drive when subjected to a bus disturbance. The results displayed include the following quantities: bus voltage (V_{bus}), integrator of the current loop (X_{qs}), current command (Iqs^*), and motor phase current (I_{qs}_fdbk). The current regulator's response to the bus disturbance results in a saturation of the controller—the current regulator's integrators "wind up." The current loop saturation results in a momentary loss of current control, which is a potentially disastrous situation. The reduction in gain associated with the sine triangle PWM's voltage error (Fig. 3) is the major contributor to this condition.

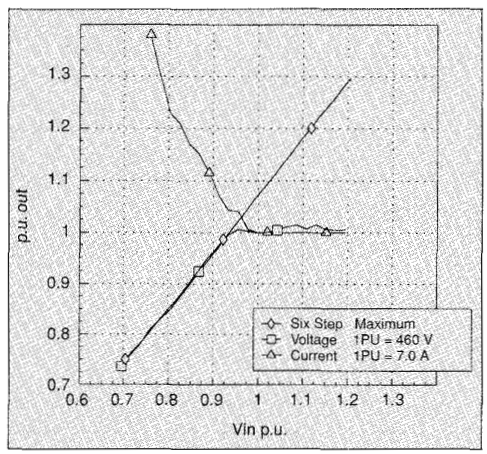

Fig. 9. V/Hz with CMT steady state characteristics—experimental.

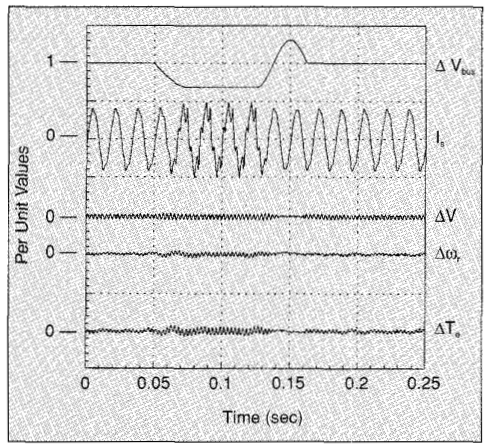

Fig. 10. V/Hz with CMT transients for bus disturbance—simulation.

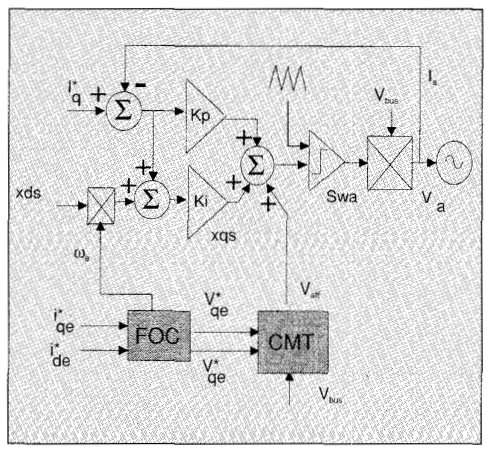

Fig. 11. FOC—CRPWM with CMT voltage feedforward.

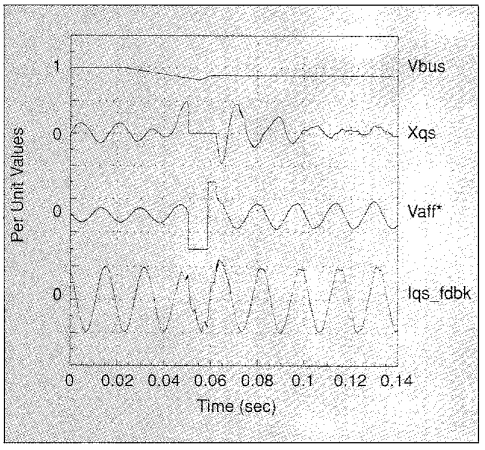

Fig. 12. FOC—CRPWM with CMT for bus disturbance—experimental.

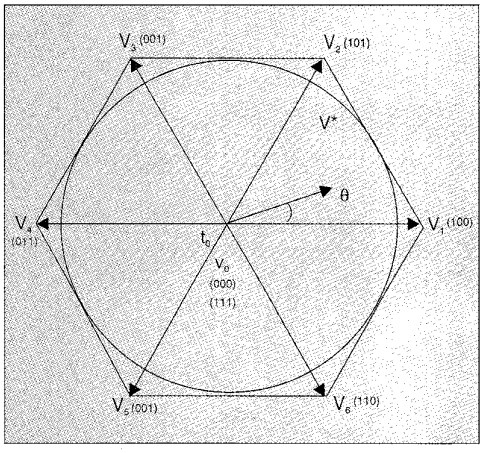

Fig. 13. Switching state vectors.

Overmodulation For PWM Inverters

The previous section demonstrated deficiencies with PWM operation in the pulse dropping region. Recently, feedforward overmodulation was shown to extend the operation of sine wave modulation well into the pulse dropping region [13]. To correct the modulator for the loss of gain and the resulting error in output voltage, a compensator was designed to amplify the modulating signal before entering the PWM generator.

As shown in [13], the compensator resulted in an approximate solution. Furthermore, although it is a noniterative technique, the compensator ($M_{i\text{-}comp}$)—repeated here as (1)—requires an on-line computation involving the voltage command (V^*) and bus voltage (V_{bus}). Clearly, the sensitivity of the calculation to the bus voltage for high modulation indices is a cause for concern.

The shaded areas of Fig. 6 show the error when employing the approximate solution of (1). Although the errors may be reduced through linear interpolation, the added complexity does not eliminate the problems inherent with the approximate method.

$$M_{icomp} = \frac{1}{\sqrt{\frac{6 - 3\pi V^*}{V_{bus}}}} \tag{1}$$

An Improved Overmodulation Strategy

To improve the performance of PWM inverters in the pulse dropping region, the authors have proposed the compensated modulation technique (CMT) [11, 12]. This new approach eliminates the errors of Fig. 6 and the complex mathematics of (1). A table lookup implementation of the CMT, which linearizes the transfer function $\frac{\hat{V}}{V^*}$, eliminates the complexity of other overmodulation strategies. Fig. 7 shows a simplified implementation of the CMT. This formulation of the compensator applies to most PWM generators—sine wave, third harmonic, space vector, and the discontinuous modulators.

The table entries for sine wave modulation are calculated off-line by solving (2) for the modulation index (M_i), thereby creating a preamplification factor equal to the inverse of the inverter's nonlinearity [10]. Fig. 8 displays the compensated modulation index (M_{CMI}) as a function of normalized incremental voltage. M_{CMI} preamplifies the modulating signal and compensates for the inverter's nonlinearity. The CMT cancels the inverter's nonlinearity when incorporated in the feedforward path of the modulator. This produces a unity transfer function for all operating regions.

$$\frac{V^*(M_i)}{V_{bus}} = \left\{ \arcsin\left(\frac{1}{M_i}\right) + \frac{1}{M_i}\sqrt{1 - \frac{1}{M_i^2}} \right\} M_i \tag{2}$$

The CMT's incremental address when applied to a sine wave modulator is given by the following equation [12]. For the other modulators, the offset $\frac{1}{2}$ is replaced by $\frac{1}{\sqrt{3}}$. $i_{\max}$ is the number of table entries.

$$\Delta V_i = \frac{V_i^*}{Vbus} = \left(\frac{V_i^*}{V_{bus}} - \frac{1}{2} \right) \frac{1}{i_{\max}} \tag{3}$$

Fig. 9 shows steady state results from an experimental investigation of the CMT applied to a V/Hz drive system. Similar to Fig. 2, the input line was varied over a wide range, and the terminal voltage was measured. In the figure, the fundamental terminal voltage and maximum six-step voltage normalized to 460 V are plotted. Unlike the results of Fig.2, the V/Hz drive of Fig. 9 shows rated voltage

Of the overmodulation techniques for voltage space vector, the method proposed by Holtz is the most lucid.

is maintained for $V_{in} > 0.95$ p.u.; below this value six-step operation is achieved.

Fig. 10 displays simulation results for an identical disturbance to that of Fig. 4. The results, however, are quite different. When the bus disturbance occurs with the CMT, the V/Hz's voltage algorithm increases the voltage output of the inverter; thus preventing the transients observed in Fig. 4. Therefore, to reject bus disturbances, the control must preamplify the modulating signal. The amount of preamplification is determined by the CMT function (Fig. 8).

The CMT also has applications in CRPWM inverter drives. Fig. 11 shows a typical implementation of the CMT with a field-oriented control (FOC). The CMT and FOC were implemented in a microprocessor-based ac drive and subjected to a bus voltage disturbance. Experimental results are shown in Fig. 12 with variables displayed as in Fig. 5 with the current command replaced with the voltage feedforward (V_{aff}).

The addition of voltage feedforward with CMT prevents saturation of the current regulator's integrator and the ensuing limit cycle of Fig. 5. In this case, the CMT amplifies the feedforward voltage through the M_{CMI} function (Fig. 8). When the bus voltage decreases sufficiently, the integrator is disabled and the control achieves six-step operation. Once the bus voltage exceeds a minimum, the integrator is activated and current control resumes. The limit cycle is eliminated and field orientation is maintained.

Comparison of Overmodulation Methods

Of the overmodulation techniques for voltage space vector, the method proposed by Holtz presented in [8] is the most lucid. In this section a comparison of the CMT and the method of Holtz is made. To facilitate this comparison, the modulation index is redefined as the ratio of the output fundamental voltage to the fundamental voltage at six-step. Thus, for sine wave modulation, overmodulation begins at $M_i = .785$.

The sine wave modulation method naturally yields continuous and smooth operation from the onset of pulse dropping to six-step by overmodulating the carrier. The CMT overmodulation strategy proposed simply linearized this saturating nonlinearity. Conversely, space vector modulation strategies do not have a natural mode of operation above a fundamental output voltage of $M_i = .906$, where $M_i = 1$ is the output voltage at six-step. This voltage limit trajectory is shown as a circle inscribing the hexagon in Fig. 13 and is characterized by every resulting vector having a zero state.

Holtz proposed two modes of overmodulation to obtain operation between this limit and six-step. Mode I ranges from $M_i = .906$ to $M_i = .951$ and produces a trajectory that is sinusoidal at angles where the space vector equations are satisfied and that traces the hexagon boundary at angles where the calculations are invalid and no zero state can be applied. The angular rate of change of the voltage vector V^* remains constant in both the hexagon and sinusoidal regions. The upper boundary of this mode is characterized by a trajectory that traces the hexagon, resulting in no zero state application.

Mode II applies from $M_i = .952$ to $M_i = 1$ and produces a trajectory that sweeps the sides of the hexagon and holds at the vertices. As voltage output increases, the trajectory sweeps the sides of the hexagon at increasingly faster rates and holds at the

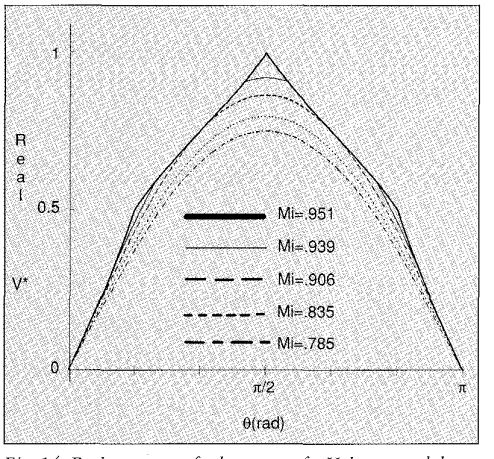

Fig. 14. Real component of voltage vector for Holtz overmodulation mode I.

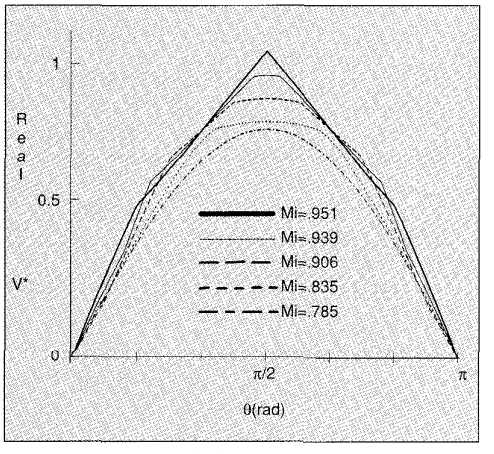

Fig. 15. Real component of voltage vector in sinewave overmodulation mode I.

vertices for increasingly longer times. In the limit the trajectory jumps from vertex to vertex, holding for one-sixth of the fundamental period, resulting in six-step operation.

The CMT modulation strategies proposed have comparable overmodulation modes to those proposed by Holtz. For sine wave modulation, however, a third mode exists from $M_i = .785$ to $M_i = .906$. In this case the modulating signal must be amplified by a factor of 1.4 to obtain the $M_i = .906$ output.

The CMT sine wave strategy requires amplification factors ranging from 1.4 to 2.0 and from 2.0 to ∞ to obtain voltages comparable to Holtz's Mode I and II, respectively. Although the resulting fundamental component voltages are comparable in both methods, it is interesting to note that the waveforms are not identical and do not have identical harmonics. Holtz selected a trajectory that traced out the hexagon with a constant rate of angular change in Mode I. The CMT strategy produces a trajectory that also traces out the hexagon, but at a rate that has a sinusoidal component to it. While

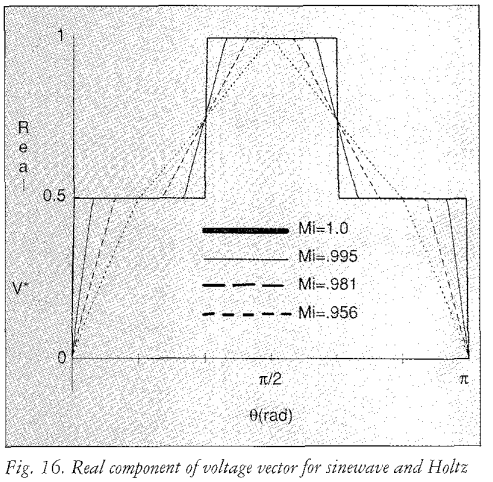

Fig. 16. Real component of voltage vector for sinewave and Holtz overmodulation mode II.

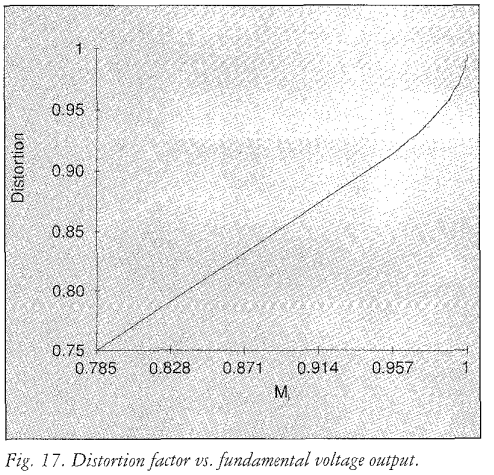

Fig. 17. Distortion factor vs. fundamental voltage output.

As the modulation index increases to unity, both overmodulation schemes exhibit an appreciable increase in distortion.

in Mode II, the CMT combines these different hexagon rates with hold times at the vertices.

Figs. 14 and 15 illustrate the Mode I differences by plotting the real component of the vector trajectory as a function of time for Holtz and sine wave CMT, respectively [8]. The real component represents the line to neutral voltage applied to the machine without the PWM switching harmonics. In Fig. 14 the trajectories are sinusoidal to $M_i = .906$ and have increased harmonics thereafter. In Fig. 15 trajectories are sinusoidal to $M_i = .785$ with increasing harmonics thereafter. Notice that although the fundamental components of the voltages are the same, the waveforms are different. Notice also that the boundary voltage in Fig. 15 (M_i=.956) is larger than that in Fig. 14 (M_i=.951). In both cases the trajectory traces the hexagon, but with the different angle modulation strategies previously discussed.

Fig. 16 shows the voltages for Mode II of Holtz and the CMT sine wave scheme. In this region of operation the two schemes are indistinguishable, culminating with the well-known six-step waveform (M_i=1.0). As the voltage increases from M_i=.956, the flat portions of voltage correspond to the trajectory being held at a vertex of the hexagon, while the sloped portions of the voltage correspond to the trajectory sweeping the hexagon. Notice how the hold times and sweep rates increase with output voltage. Holtz programmed hold angles to produce these voltages while the sine wave scheme naturally generated similar waveforms.

Although the voltage waveforms in Mode I of Holtz are different from those in the sine wave CMT scheme, the additional harmonics generated by both techniques are indistinguishable. Fig. 17 illustrates the harmonic distortion of the voltages as a function of the fundamental output voltage. The RMS voltage for each technique is normalized to the RMS of the six-step voltage waveform. For modulation indices from .785 to .906, both modulation schemes have a linear rise in the distortion factor. This suggests marginal differences between sine wave overmodulation and the extended linear region provided by space vector modulation. Further increases in the modulation index, from .907 to .951, show a slight increase in the rate of increase in distortion for both modulation schemes. Finally, as the modulation index increases to unity, both overmodulation schemes exhibit an appreciable in-

crease in distortion, culminating in a distortion factor of unity at six-step.

Summary

We have reviewed technical issues affecting the performance of PWM voltage source inverter drives. Until now, the transition from PWM to six-step operation was an unresolved problem limiting the performance of ac drive systems. Experimental results from commercially available V/Hz drives showed their inability to deliver commanded voltage for typical line variations. Furthermore, this article demonstrates the performance degradation that occurs when CRPWM inverters operate in the overmodulation region.

We have described a recently developed overmodulation strategy—the Compensated Modulation Technique (CMT). Results presented show the CMT solves the problems with V/Hz and CRPWM drives by linearizing the voltage transfer function for the entire operating region.

We have also compared the CMT with another recently developed overmodulation strategy. Although both strategies have essentially identical distortion characteristics, the CMT provides the unique ability to transition all modern modulation techniques.

Acknowledgment

The authors wish to acknowledge the technical assistance of Mr. D. Schlegel during this research.

References

[1] A. Schonung and H. Stemmler, "Static Frequency Changers with Subharmonic Control in Conjunction with Reversible Variable Speed AC Drives," *Brown Boveri Rev.*, pp. 557-577, 1964.

[2] D.A. Grant, "Technique for Pulse Dropping in Pulse-Width Modulated Inverters," *IEE Proc.*, vol. 128, Pt. B, no. 1, January 1981, pp. 67-72.

[3] A.B. Plunkett, "A Current-Controlled PWM Transistor Inverter Drive," *IEEE IAS Annual Meeting Conference Record*, pp. 785-792, 1979.

[4] Y. Murai, T. Watanabe, and H. Iwasaki, "Waveform Distortion and Correction Circuit for PWM Inverters with Switching Lag-Times," *IEEE Trans. on Industry Applications*, vol. IA-23, no. 5, September/October 1987, pp. 881-886.

[5] N. Mutoh, A. Ueda, K. Sakai, and K. Nandoh, "Stabilizing Control Method for Suppressing Oscillations of Induction Motors Driven by PWM Inverters," *IEEE Trans. on Industrial Electronics*, vol. 37, no. 1, February 1990, pp. 48-56.

[6] T.M. Rowan and R.J. Kerkman, "A New Synchronous Current Regulator and an Analysis of Current-Regulated PWM Inverters," *IEEE Trans. on Industry Applications*, vol. IA-22, no. 4, July/August 1986, pp. 678-690.

[7] J. Holtz, "Pulsewidth Modulation—A Survey," *IEEE Trans. on Industrial Electronics*, vol. 39, no. 5, October 1992, pp. 410-420.

[8] J. Holtz, W. Lotzkat, and A. Khambadkone, "On Continuous Control of PWM Inverters in the Overmodulation Range Including the Six-Step Mode," IECON, 18th Ann. Conf., IEEE Ind. Electronics Soc., San Diego, 1992, pp. 307-312.

[9] G. Griva, T.G. Habetler, F. Profumo, and M. Pastorelli, "Performance Evaluation of a Direct Torque Controlled Drive in the Continuous PWM-Square Wave Transition Region," Power Electronics Specialists Conference, Seattle, WA, 1993, pp. 237-234.

[10] T.M. Rowan, R.J. Kerkman, and T.A. Lipo, "Operation of Naturally Sampled Current Regulators in the Transition Mode," *IEEE Trans. on Industry Applications*, vol. IA-23, no. 4, July/Aug. 1987, pp. 586-596.

[11] R.J. Kerkman, D. Leggate, B.J. Seibel, and T.M. Rowan, "Inverter Gain Compensation for Open Loop and Current Regulated PWM Controllers," International Association for Mathematics and Computers in Simulation (IMACS), 4th International Conference, July 7-9, 1993, pp. 7-12.

[12] R.J. Kerkman, D. Leggate, B.J. Seibel, and T.M. Rowan, "An Overmodulation Strategy for PWM Voltage Inverters," IECON '93, 19th International Conference on Industrial Electronics, Control, and Instrumentation, November 15-19, Maui, Hawaii, pp. 1215-1221.

[13] R.J. Kerkman, B.J. Seibel, D.M. Brod, T.M. Rowan, and D. Leggate, "A Simplified Inverter Model for On-Line Control and Simulation," *IEEE Trans. on Industry Applications*, vol. 27, no. 3, May/June 1991, pp. 567-573.